# ML Mule: Mobile-Driven Context-Aware Collaborative Learning

## Haoxiang Yu

hxyu@utexas.edu University of Texas at Austin Austin, Texas, USA

## **Javier Berrocal** jberolm@unex.es

University of Extremadura Badajoz, Badajoz, Spain

## Christine Julien christinejulien@vt.edu Virginia Tech Blacksburg, Virginia, USA

#### **Abstract**

Artificial intelligence has been integrated into nearly every aspect of daily life, powering applications from object detection with computer vision to large language models for writing emails and compact models in smart homes. These machine learning models cater to individual users but are often detached from them, as they are typically stored and processed in centralized data centers. This centralized approach raises privacy concerns, incurs high infrastructure costs, and struggles with personalization. Federated and fully decentralized learning methods have been proposed to address these issues, but they still depend on centralized servers or face slow convergence due to communication constraints. To overcome these challenges, we propose ML Mule, a approach that utilizes individual mobile devices as "Mules" to train and transport model snapshots as they move through physical spaces, sharing these models with the physical "Spaces" they inhabit. This method implicitly forms affinity groups among devices associated with users who share particular spaces, enabling collaborative model evolution, and protecting users' privacy. Our approach addresses several major shortcomings of traditional, federated, and fully decentralized learning systems. The proposed framework represents a new class of machine learning methods that are more robust, distributed, and personalized, bringing the field closer to realizing the original vision of intelligent, adaptive, and genuinely context-aware smart environments. The results show that ML Mule converges faster and achieves higher model accuracy compared to other existing methods.

## **CCS** Concepts

• Computing methodologies → Machine learning; Artificial intelligence; • Human-centered computing  $\rightarrow$ Ubiquitous and mobile computing theory, concepts and paradigms.

## **Keywords**

Knowledge Transfer, Internet of Things, Federated Learning, Decentralized Learning, Mobile Computing

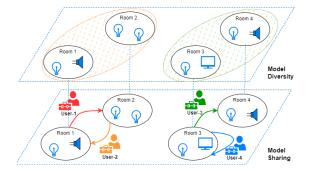


Figure 1: Example of ML Mule sharing process

## Introduction

AI-driven technologies are transforming modern life, streamlining processes and embedding themselves into everyday routines. Individuals interact with machine learning models constantly—whether turning on lights with a virtual assistant in the morning, composing emails using ChatGPT at work, tracking calories burned with a smartwatch, or letting a smart thermostat adjust the temperature before sleep. These interactions demonstrate how deeply machine learning models are integrated into our lives, yet the way these models operate often falls short of realizing the vision of truly "smart" environments.

Most machine learning models used in these applications are trained, stored, and executed on centralized servers far removed from the end users they support and the smart environments they control. While this remote infrastructure enables powerful computation and scalability, it also introduces significant challenges. Centralized systems pose risks to user privacy, have high infrastructure costs, and struggle to dynamically adapt to the needs of individual users. Moreover, they fail to provide the contextual intelligence and adaptive behavior that are key features of a genuinely smart environment. The rapid advancement of generative AI, which often relies on even larger and more complex models, further highlights these limitations, as the need to balance privacy, scalability, and real-time adaptation becomes increasingly critical. In an ideal scenario, machine learning models would remain closer to users, learning and evolving

directly from their unique experiences and interactions over time

To address some of these limitations, researchers have proposed federated learning, a paradigm in which devices train models on local data and periodically share updates to build a global model [1]. While federated learning mitigates some privacy concerns by retaining data on devices, it still assumes (1) constant internet connectivity and (2) the existence of a single, unified model to capture all user behaviors. These assumptions are often impractical in real-world settings, where devices may only have intermittent internet access, and diverse users in distinct environments may require specialized models. In addition, federated learning fails to be contextaware within the model application environment, as it is not embedded in and tailored to the environment where the models are used, and the server aggregates the model purely based on the model itself or a few simple data points.

Fully decentralized approaches, such as Gossip Learning [2] and Opportunistic Collaborative Learning (OppCL) [3], eliminate the need for centralized aggregation servers by enabling devices to exchange model updates directly during peer-to-peer encounters. However, these methods heavily rely on opportunistic and often unpredictable communication patterns, limiting their feasibility. Moreover, decentralized approaches frequently suffer from slow convergence rates due to sparse and intermittent device encounters, as well as challenges posed by heterogeneity in device environments and user behaviors.

From a holistic perspective, federated learning approaches require collaborators to be coupled in time (i.e., all connected to the Internet simultaneously), while decentralized approaches require collaborators to be coupled in both space and time. However, to the best of our knowledge, no existing approaches require coupling only in space. In this work, we propose a distributed machine learning approach that utilizes the spatial mobility of users and their devices as they naturally transition between different physical space to address these limitations. Our novel insight is that coupling in space, even when decoupled in time, elevates the impact of the space that the models represent. Such representation enables a particular subset of applications where the space has particular importance to what the model learns. Our framework identifies the principal actors using two key roles: (1) fixed devices embedded in physical spaces, and (2) mobile devices carried by users. When a mobile device enters a space with fixed devices, they collaboratively train a model using locally acquired data. The trained model is then stored on both the fixed and mobile devices. As the user moves to new spaces, the mobile device carries a snapshot of the model, sharing it with fixed devices in the new environment. Similarly, fixed devices share their snapshots with any newly arrived mobile devices that enter the space.

Figure 1 illustrates an example of *ML Mule* in a smart home control setting. Fixed devices, such as smart lights and speakers, collaborate with mobile devices carried by users to train and exchange model snapshots. For instance, User-1 (red) trains a model in Room 1, carries it to Room 2, and shares it with the fixed devices in Room 2. Similarly, User-2 (orange) and other users transport model snapshots between rooms, enabling fixed devices in different rooms to adapt their models collaboratively. In this figure, User-1 and User-2 frequently enter Rooms 1 and 2, sharing similar characteristics. Likewise, User-3 (green) and User-4 (blue) interact between Rooms 3 and 4, sharing similar characteristics with each other but different from those of Users 1 and 2 in Rooms 1 and 2.

This framework creates a dynamic and collaborative learning ecosystem in which mobile devices act as mules, a term inspired by its use in delay-tolerant network, where mules refer to mobile agents that transport and exchange data between disconnected nodes [4]. Similarly, in our proposed ML Mule framework, mobile devices are transporting and exchanging model updates between physical spaces. By implicitly forming affinity groups among devices that overlap by virtue of their shared spaces, our approach enables localized and context-aware learning through aggregation of models that incorporate contextual information. This collaborative learning mechanism presumes that users who share physical spaces are likely to exhibit similar characteristics, enabling the creation of more nuanced, personalized, and adaptive models that can be tailored to how these users use the spaces they inhabit.

ML Mule is not a wholesale replacement for all use cases suited to federated learning or decentralized learning. Instead, it is designed to address specific applications where this approach provides clear advantages, while other applications may continue to benefit from existing methods. The particular use cases for which ML Mule is particularly fitting are those where the space significantly influences the learning task. These include, for example, applications in smart environments, where devices in the space attempt to learn how to configure themselves to support the users in that space. Human activity recognition applications are another example — different humans often perform the same or similar activities in the same space (e.g., a gym, a restaurant or a move).

Our work represents a step forward in achieving distributed machine learning systems that are robust, realistic, privacy-preserving, and tailored to individual needs. In summary, the main contributions of this paper include:

(1) We introduce *ML Mule*, a mobile-driven, contextaware collaborative learning approach that leverages user mobility to transport and update models among

- fixed devices, eliminating the need for stable or centralized network connections.
- (2) We validate ML Mule on two distinct tasks—image classification (CIFAR-100 [5]) and human activity recognition (EgoExo4D [6]), demonstrating that the framework can handle diverse data distributions and modalities under limited or intermittent connectivity.
- (3) We show that *ML Mule* consistently outperforms or matches existing methods—including FedAvg [7], FedAS [8], CFL [9], Gossip Learning [2], and Local Only—across different data distributions (Dirichlet [10] and Shards) under diverse mobility patterns.

The remainder of this paper is organized as follows: Section 2 reviews related work and highlights key challenges. Section 3 details the system design and underlying architecture of *ML Mule*. Section 4 presents the evaluation methodology and results, including comparisons with existing methods. Finally, Section 5 concludes the paper by discussing the limitations of *ML Mule* and outlining potential directions for future research.

#### 2 Related Work

During the last few years, the research community has been working on improving the behavior of smart environment to automatically adapt their behavior to user's needs and preferences. Concretely, relevant background work has two related components: (1) distributed learning; (2) intelligent context-aware environments.

**Distributed learning** is a machine learning method that attempts to address the disadvantages of traditional machine learning. It can be separated into two subcategories: federated learning (FL) and fully decentralized learning. Compared to traditional machine learning that shares data between a server and end users, federated learning keeps the data with the user. The user trains the model locally and shares updates to the model with the server [1]. The server can then aggregate model updates from multiple users' devices using various aggregation methods, such as FedAvg [1], FedAS [8], CFL [9], etc. In contrast, fully decentralized learning functions without a central aggregation server and evolves the model with each encounter between any two mobile devices. An example method in this category is Gossip Learning [2], which conducts an exchange-aggregate-training cycle at every encounter, while Opportunistic Collaborative Learning [3] conducts an exchange-training-exchangeaggregate cycle on every encounter.

Different from traditional FL, which aims to train a single global model collaboratively across multiple clients, Personalized Federated Learning (pFL) attempts to provide a personalized model or a base model that individuals can

easily adapt to with few-shot learning [11]. Common methods to address this include model decoupling, which splits the model structure into a shared global part (e.g., a feature extractor or backbone) and a personalized local part (e.g., task-specific classifier layers) [12], or using two models—one shared and one that remains purely local [13]; meta-learning approaches that focus on finding an initial shared model that can be easily adapted to users' local datasets with one or a few gradient descent steps [14, 15]; adjusting the regularization function at the aggregation steps [16]; or using a low-rank decomposition to decouple general knowledge (shared among clients) and client-specific knowledge [17].

However, existing approaches to FL and pFL require a centralized aggregation server to coordinate aggregation, which can face single-point-of-failure issues and has high infrastructure costs in terms of computation and communication. In addition, it assumes constant internet connectivity, which is often impractical in real-world settings, where devices may only have intermittent internet access. On top of these federated learning challenges, existing personalized federated learning research is theoretical and focused on aggregation method and model selected, failing to utilize the dynamics of the end user and spatiotemporal context to improve model performance. Fully decentralized approaches eliminate the need for centralized aggregation servers by enabling devices to exchange model updates directly during peer-to-peer encounters. However, these methods heavily rely on opportunistic and often unpredictable communication patterns, limiting their feasibility. Moreover, decentralized approaches frequently suffer from slow convergence rates due to sparse and intermittent device encounters, as well as challenges posed by heterogeneity in device environments and user behaviors. In addition, the existing decentralized learning research remains largely theoretical as well and has not seen widespread real-world deployment due to communication constraints [18].

Intelligent context-aware environments are systems that sense, interpret, and respond to contextual information (e.g., user preferences, environmental conditions, temporal factors) to deliver personalized, adaptive services. The machine learning method used in such an environment is called Context-Aware Machine Learning. This approach highlights the diverse nature of contextual information and its relevance across spatio-temporal domains [19]. Harries et al. claim that one of the most important aspects of Context-Aware Machine Learning is understanding hidden properties that change over time. In the real world, a good machine learning model should not only perform good classification with the available data, but also detect changes in the hidden properties and update the model accordingly [20]. Sarker et al. categorize context into external or physical context, including location, time, light, movement, etc., and internal

or logical context, such as a user's interaction, goal, and social activity [21]. Such machine learning methods are useful across different domains, such as computer vision [22], human activity recognition [23], smart home control [24], autonomous and smart transportation [25], etc. [26, 27, 28].

Modular Machine Learning methods are commonly used in Context-Aware Learning [25]. They aim to break the problem into different components, solve them with different models, and combine the results into a final solution [29]. This breakdown method can be split into data modularity, which modularizes input for deep learning models; task modularity, which breaks down the task into sub-tasks and develops sub-models to address each problem individually; and model modularity, which focuses on the machine learning model itself [30]. Model modularity can be split into hybrid, ensemble, and graph-based Machine Learning [25]. In the hybrid method, researchers use two deep learning architectures and merge them in the final output [31]. Omolaja et al. developed context-aware human activity recognition models using a hybrid approach that utilizes light conditions and environmental noise levels with IMU signal data to predict the activity the user is performing [32]. Ensemble methods are similar to hybrid methods, but the only difference is that the hybrid method directly combines the network, whereas the ensemble method post-processes multiple independent model outputs [30]. Bejani et al. proposed a CADSE system to design a driving style evaluation system using an ensemble method with smartphone sensors and context data. In their proposed system, the result is an ensemble of car, traffic, and maneuver classification modules [33]. The graph-based context-aware method is widely used in recommendation algorithms. For example, Wu et al. designed a graph-based multi-context-aware recommendation algorithm that uses neighborhood aggregation based on an attention mechanism with local context to enhance the representations of users and items [34].

Mobile phones are among the most important devices for context-aware machine learning because they record detailed individual contextual data, including where, when, and with whom users interact during their daily activities [21, 30], and they also have sufficient computational power for deep model training and inference [18]. However, existing efforts do not effectively use such mobile information, often treating context-awareness as an additional weight in the model, which is ineffective. For example, a model used in a desert does not need information on how to handle rain. In addition, Brdiczka claims that a successful relationship between humans and AI requires meeting users' expectations in diverse environments and maintaining full control over AI systems [35]. The former aligns with context-aware machine learning, which adapts to varying contextual information to

provide personalized services. The latter matches the principles of distributed and collaborative learning, where data remains on the user's device, granting users maximum control over their models and enhancing privacy.

While federated and decentralized learning address some drawbacks of traditional machine learning, they still face practical barriers such as heavy reliance on stable network infrastructure or slow convergence in opportunistic settings. Simultaneously, context-aware machine learning underscores the importance of adapting to users' diverse real-world conditions but often treats context as a mere additional feature rather than an integral part of model design or data distribution. Thus, existing solutions fall short of leveraging the spatial mobility of users and device interactions in a way that marries both decentralized and context-aware principles.

## 3 System Design

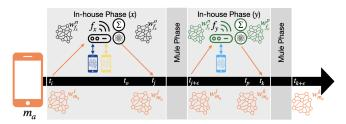
To address the challenges listed above, we propose *ML Mule*, a mobile-driven context-aware collaborative learning approach that utilizes individual users and their mobile devices as *Mules* to carry models between different physical spaces, exchanging and evolving the models with fixed devices located in those spaces.

In the *ML Mule* architecture, two categories of devices are involved: mobile devices  $(m_a)$ , which are accompany with users and can move between rooms or spaces, thereby acting as mules that carry the model across different locations; and fixed devices  $(f_i)$ , that are stationary devices deployed in specific rooms or spaces. We denote the set of all mules as M the set of all fixed devices as F.

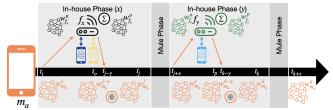
The system provides three main functionalities:

- (1) **Mule**: A mobile device  $m_a$  that carries the model w from  $f_i$  to  $f_j$ . We donate this operation by  $mule(w, m_a, f_i, f_j)$ .
- (2) Hosting: fixed device f<sub>i</sub>, stores the model w and allows other devices to access it (denoted by host(w, f<sub>i</sub>))
- (3) **Local Training**: Depending on the data location, the training can be performed either on a mobile device  $m_a$  (donated by  $train_{m_a}(w)$ ) or on the fixed device  $f_i$  (donated by  $train_{f_i}(w)$ ).

Figure 2 illustrates the overall architecture of the system. Subfigures 2a and 2b show two major phases of the proposed system, the *in-house* phase and the *mule* phase, which will be explained in more detail later in this section. Both figures are drawn with one mobile device  $m_a$  at their center: the mobile device  $m_a$  enters the space of the fixed device  $f_x$ , evolves the model with  $f_x$ , leaves the space, and carries the model  $w_a^j$  to  $f_y$  ( $mule(w_a^j, m_a, f_x, f_y)$ ), then evolves the model with  $f_y$ , and continues this procedure. At the same time, other devices are interacting with  $f_x$  and  $f_y$  as well.



(a)  $f_X \in F$  and  $f_y \in F$  training scenario. New data is collected on the fixed devices F. The mobile device  $m_a \in M$  shares the model with  $f_X \in F$ , receives updates, mules to  $f_y \in F$ , and repeats the process. Each  $f_X \in F$  and  $f_y \in F$  both aggregate and train the model upon receiving it from  $m_a \in M$ .



(b)  $m_a \in M$  training scenario. New data is collected on the mobile device  $m_a$ . The device shares the model with  $f_x \in F$ , receives the aggregated version, performs on-device training with its local data, then mules the updated model to  $f_y \in F$  and repeats. In this mode,  $f_x \in F$  and  $f_y \in F$  only aggregate the model rather than training.

Figure 2: Illustration of the two main training modes. In (a), the main training occurs on fixed devices F; in (b), training takes place on the mobile devices M.

The major difference between subfigure 2a and 2b is that in subfigure 2a, the model training is completed on fixed devices  $f_x$  ( $train_{f_x}(w)$ ) and  $f_y$  ( $train_{f_y}(w)$ ), while in subfigure 2b, the model is trained on the mobile device  $m_a$  ( $train_{m_a}(w)$ ). This difference arises because training is intended to happen on the devices that collect the data, but the data location depends on the downstream task. For example, if the downstream task is human activity recognition, the mobile devices M conduct the training since the data is generated on those devices. Conversely, if the downstream task is smart home control, the fixed devices F may have more information about the user's actions, so they conduct model training.

As shown in Figure 2, ML Mule involves several interconnected steps. At the beginning, each mobile device  $(m_a \in M)$  continuously detects any fixed device  $(f_a \in F)$  through shortrange communication protocols such as Bluetooth, Wi-Fi Direct, or other network discovery mechanisms [36], and vice versa (i.e.,  $Discover(m_a)$  and  $Discover(f_a)$ ). When both devices discover each other at time t, we consider  $m_a$  and  $f_a$  to be co-located, represented as  $c = \langle m_a, f_a, t \rangle$ . The set of all co-location events is  $C = \{c\}$ , and we use  $C[m_a, t_1, t_2]$ 

to denote all co-location events involving the mule  $m_a$  that occur in the time window  $[t_1, t_2]$ ,  $C[f_a, t_1, t_2]$  to denote all co-location events involving the fixed device  $f_a$  in the same time window, and  $C[f_a, m_a]$  to denote all co-location events involving the mule  $m_a$  and fixed device  $f_a$ .

#### 3.1 In-House Phase

*ML Mule*'s **In-House Phase** begins when devices  $m_a$  and  $f_a$  are co-located. Specifically, if  $\exists (c = \langle m_a, f_\alpha, t_i \rangle)$  such that  $\nexists (c = \langle m_a, f_\alpha, t_{i-1} \rangle)$ , *ML Mule* identifies time  $t_i$  as the point of initial contact between the mule  $m_a$  and the fixed device  $f_a$ . At this point in time, *ML Mule* kicks off one of two versions of its training process.

**Fixed Device Training**. For applications where fixed devices collect data and perform local training, the discovery event initiates a *share-aggregate-train-share* cycle. In this process, the devices complete the following steps, in order:

- (1)  $m_a$  sends its local model weights to  $f_a$  (denoted as  $sent(m_a, f_a, w)$ )
- (2)  $f_a$  aggregates the received model with its own model (see the discussion of the aggregation process, below)
- (3)  $f_a$  performs  $train_{f_a}(w)$  using  $f_a$ 's local data
- (4)  $f_a$  sends the updated model weights back to the mobile device  $m_a$  ( $sent(f_a, m_a, w)$ )
- (5)  $m_a$  aggregates the received model with its own (see the discussion of the aggregation process, below)

**Mobile Device Training.** Alternatively, the discovery event may trigger other applications to perform training on the mobile device (i.e., the mule). In this case, the devices perform a *share-aggregate-share-train* cycle, completing the following steps:

- (1)  $m_a$  sends its local model weights to  $f_a$  ( $sent(m_a, f_a, w)$ )
- (2)  $f_a$  aggregates the received model with its own model (see the discussion of the aggregation process, below)
- (3)  $f_a$  sends the aggregated model weights back to  $m_a$  (sent( $f_a$ ,  $m_a$ , w))
- (4)  $m_a$  aggregates the received weights with its own
- (5)  $m_a$  trains the aggregated model using its local data  $(train_{m_a}(w))$

The first two steps in this second process are the same as in the Fixed Device Training approach; they serve to ensure that the mule leaves a record of having visited the space so that other mules that arrive can learn from this mule's prior experiences. This is how *ML Mule* achieves coupling in space while also achieving *decoupling* in time.

**Model Aggregation Operations.** Several steps above rely on aggregating the weights of two models to generate an updated version of the model.

During each co-location of a mobile device  $m_a$  with a fixed devices  $f_a$ , multiple training cycles may occur. Since neither device knows when the current co-location will end, they

continuously execute the following sequence: 1) the device training pipeline as described in the previous paragraphs; 2) wait for a constant delay d (i.e., a user-defined or dynamically adjustable parameter); and 3) repeat for as long as  $m_a$  remains co-located with  $f_a$ . As a result, dwell time directly influences the final aggregation weights, as devices that stay longer in a space will engage in more training cycles and more frequent parameter exchanges, thereby having a greater impact on the model evolution. In this work, we use a weighted averaging method [37] to aggregate the models, as such methods have been widely adopted by the research community. However, it can be easily replace with other aggregation methods, such as FedDyn [38], SCAFFOLD [39], or FedProx [40]. Other styles of aggregation could also consider incorporating the amount of data or the quality of the model, as presented in [41].

## 3.2 Mule Phase

ML Mule's Mule Phase is much simpler. It begins when the mobile device  $m_a$  physically leaves the previous environment, which is defined as  $m_a$  no longer detecting  $f_a$  via shortrange communication protocols. During the Mule Phase,  $m_a$  holds the most updated model it received in the previous Inhouse Phase and continues discovering other fixed devices  $f_b \in F$   $(mule(w, m_a, f_a, f_b))$ . Once new devices are detected, the next In-house Phase begins.

Meanwhile, if there is no  $m \in M$  detected by a fixed device  $f_a \in F$ , then  $f_a$  will hold the model  $(host(w, f_a))$  until the next  $m \in M$  is detected, triggering another In-house Phase.

## 4 Evaluation

In this section, we answer the following research questions:

- (1) Does *ML Mule* achieve competitive convergence speed and final accuracy compared to existing distributed learning paradigms?
- (2) How do different mule mobility patterns affect the overall model accuracy and convergence rate?
- (3) Does the distribution of data across mobile and fixed devices influence learning outcomes and system stability?
- (4) How does *ML Mule* adapt its performance (e.g., model convergence time, final accuracy) across different downstream tasks with varying data modalities and complexities?

## 4.1 Experiment Design

To address the research questions listed above and evaluate the performance of *ML Mule*, we design three experiments employing the CIFAR-100 dataset [5] and the EgoExo4D dataset [6], along with three different mobility patterns. The

**first experiment** focuses on the fixed-device training scenario  $train_{f_a}(w)$  (illustrated in Figure 2a), aiming to answer research questions Q1 through Q3 under the setting that  $f_a \in F$  conducts model training. In contrast, the **second** and **third experiments** involve the mobile-device training scenario  $train_{m_a}(w)$  (as shown in Figure 2b). These latter experiments utilize two distinct datasets to address all research questions when  $m_a \in M$  is responsible for training.

Time in the simulation is defined as a 'time step', which serves as the basic unit for measuring all actions. In all experiments, the mobility patterns are generated via a random-walk approach. Each device moves freely within a space, making one move per time step. We introduce a parameter  $P_{cross}$  that controls the probability of leaving the current space. This design simulates real-world human interactions in which a user or device remains in one area for a certain amount of time before moving elsewhere.

In each simulation, there are two square areas that are completely isolated from one another, i.e., devices cannot communicate across the isolated areas. Within each area, we define *four spaces*, and we assume there are 8 *fixed devices*  $f_a \in F$  (one deployed in each space). The central space of the area remains empty and does not belong to any of the four designated subspaces.

Such a design is intended to mimic real-world mobility patterns, where users may: (1) directly move from one room to another (cross spaces directly); (2) leave one space, traverse an open space, and enter another space (cross spaces via central empty area); or (3) interact exclusively within certain spaces (e.g., in Area 0) without ever entering other spaces (e.g., in Area 1).

An example of the random-walk pattern, under three different values of  $P_{cross}$ , is presented in Figure 3. Each trajectory is colored based on the device's starting location and illustrates how devices traverse different spaces, with start points (circles) and end points (crosses) indicated in each subfigure.

We assume that the fixed devices ( $f_a \in F$ ) are installed at the center of each space and can, and only can, communicate with devices within their respective spaces via peer-to-peer methods.

### 4.2 Evaluation with Fixed-Device Training

We begin by evaluating the performance of ML Mule when model training is conducted on fixed devices ( $f_a \in F$ ). We use the CIFAR-100 dataset [5] along with the mobility patterns described above. To provide a comprehensive comparison, we benchmark ML Mule against four baselines:

FedAvg [7]: A traditional federated learning algorithm

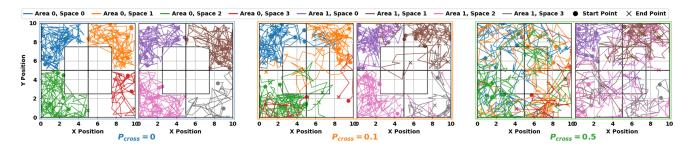


Figure 3: Example random-walk trajectories under three different crossing probabilities,  $P_{cross} = \{0, 0.1, 0.5\}$ . Each subfigure shows device movements in a 2D space partitioned into four spaces within two isolated areas. The black grid lines mark the boundaries between spaces, while circles and crosses denote start and end points for each mobile devices, respectively. A higher  $P_{cross}$  value indicates an increased likelihood that devices will leave their current space.

- FedAS [8]: A recently proposed personalized federated learning approach
- CFL [9]: A clustered federated learning method
- Local-only: Each device trains locally without any communication

4.2.1 Experimental Setup. CIFAR-100 comprises 20 superclasses and 100 classes, with each super-class containing exactly 5 classes. In our experiments, we use these 20 superclasses as the classification targets. We distribute the dataset in 5 distinct ways, including independent and identically distributed (i.i.d.) and non-iid as illustrated in Figure. 4.

The first three non-iid distributions employ a Dirichlet-based partitioning scheme [10], where smaller  $\alpha$  values typically yield a distribution closer to iid setting. The fourth distribution is adapted from the Shards approach used in the original FedAvg paper [7]. To better reflect real-world conditions, we further split the subclasses across different spaces. First, we evenly divide the 20 super-classes between Area 0 and Area 1, ensuring no overlap. Within each area, we then assign exactly 1 subclass of a given super-class to each of the four spaces (again with no overlap). For instance, if Area 0 contains the "vehicles 1" super-class, then: Space 0 in Area 0 might contain only the "bicycle" subclass; Space 1 might contain only "bus" subclass; etc. Since each super-class has 5 subclasses, and we define only four spaces, the fifth subclass is omitted in this particular setup.

In this experiment, we design a lightweight convolutional neural network (CNN) for efficient training in resource-constrained environments. The architecture features a feature extractor with two convolutional blocks (3×3 convolution, batch normalization, ReLU activation, and pooling) and a classifier with two fully connected layers.

During the simulation, all baseline federated learning methods collect models from their respective clients and subsequently perform aggregation and send the global model back to clients. We assume that model sharing is completed within one time step and define this process as one round of model evolution. For ML Mule, however, due to the opportunistic nature of encounters and peer-to-peer communication, model exchange does not happen instantly and is generally slower than the internet. We assume that sharing a model takes three time steps. Defining such a round is more challenging. In this experiment, we deploy 20 mobile devices in the environment and define one round of model evolution as 20 successful peer-to-peer model exchanges. Due to the nature of peer-to-peer communication, some devices may not enter any space during every round. The 20 peer-to-peer model exchanges might not involve every device, and some devices might communicate more than once. Meanwhile, in the Local-only method, each device does not communicate with any other device; thus, one round of training on each devices is one round of model evolution.

In all experiments, we use 20% of the data on each fixed device as a testing dataset to test how the model would perform in the space; this testing data is excluded from all training steps. Prior to the simulation, the model is pretrained on its assigned training data until the testing accuracy stops improving. The performance has been evaluated after the model returned to the fixed devices, and was retrained for 1 epoch with local training data as a fine-tuning step, evaluated on its testing data, and accuracy was used as the primary metric to evaluate the model's performance.

4.2.2 Results and Discussion. Because we employ an extrasmall CNN (to accommodate the resource constraints of mobile devices), centralized training on the CIFAR-100 superclass classification task only achieves approximately 54.12% accuracy. Table 1 summarizes the performance of our proposed approach under an i.i.d. data distribution. Although ML Mule achieves slightly lower accuracy than other federated learning methods, it remains comparable, which is expected given its inability to exchange models across the physically isolated simulation areas.

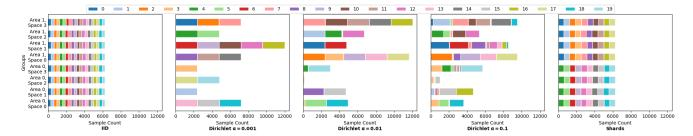


Figure 4: CIFAR-100 Data Distributions Across Different Partitioning Methods. The first subplot show IID distribution. Next three subplots illustrate Dirichlet-based distributions with  $\alpha=0.001$ ,  $\alpha=0.01$ , and  $\alpha=0.1$ . The last subplot shows our adapted Shards method, wherein super-classes are split between two areas (Area 0 and Area 1), and each space within an area contains exactly one subclass.

Table 1: Accuracy Comparison Under Fixed-Device training scenario with iid data distribution. The columns show accuracy at various rounds of model evolution (100, 200, 900). The top rows list baseline methods, while the bottom rows display results for *ML Mule* at crossing probabilities  $P_{cross} = 0, 0.1, 0.5$ . Values represent average test-set accuracy (%). Higher is better.

	Independent and identically distributed (IID)										
Round		100			200		900				
CFL [9]		48.54			50.84			53.82			
FedAS [8]		48.12			51.45			53.93			
FedAvg [7]		48.71			51.75			53.82			
Local Only	39.82				38.31			36.14			
$P_{cross}$	0	0.1	0.5	0	0.1	0.5	0	0.1	0.5		
ML Mule	38.28	38.34	35.54	41.18	43.18	41.71	47.22	51.47	51.45		

Unlike other federated learning methods that depend on cloud connectivity and robust network infrastructure, ML Mule evolves models exclusively through local, peer-to-peer exchanges. This approach provides a significant advantage in real-world environments with intermittent or nonexistent internet access. ML Mule consistently outperforms the Local Only method, which, aside from ML Mule, may be the only viable option when stable or high-speed internet is unavailable. These advantages are particularly valuable in environments with limited connectivity, simplifying the deployment and setup of devices. For instance, a small, lowcost device (e.g., a Raspberry Pi) could be deployed without internet setup or additional configuration. Using ML Mule, the model would still evolve through opportunistic encounters with mobile devices, ensuring continuous improvement even in disconnected settings.

Table 2 summarizes the accuracy at different numbers of rounds (100, 200, and 900) achieved by each method—CFL [9], FedAS [8], FedAvg [7], Local Only, and our ML Mule—under various data distributions (Dirichlet with  $\alpha \in \{0.001, 0.01, 0.1\}$  and Shards). Because ML Mule relies on the

mobility patterns of the mobile devices, the bottom rows indicate *ML Mule*'s accuracy under three different mobility patterns,  $P_{cross} \in \{0, 0.1, 0.5\}$ .

As we assume each fixed device's model is used within its space, accuracy is evaluated on a dataset matching that area's data distribution. By incorporating an additional training round (fine-tuning) after the model is returned to each fixed device, the model becomes more specialized to its local data, potentially achieving even higher accuracy than a globally optimized model. However, such a locally specialized model may not reflect the *global* optimum, since what is optimal globally may be different than what is optimal locally.

In these evaluations, a larger value for Dirichlet  $\alpha$  implies a more non-i.i.d.ness. Figure 4 reveals that varying  $\alpha$  also changes the number of categories each fixed device must specialize in. For instance, in area 1, space 3, when  $\alpha=0.001$  the local model may only need to differentiate 3 classes, whereas with  $\alpha=0.01$ , it must handle 5 classes, 9 classes for  $\alpha=0.1$ , and 10 classes for the Shards method, thereby increasing the task's complexity and reducing model performance across all methods. Turning to the i.i.d. data scenario, the model must recognize all 20 classes, making it the most demanding setting. Unsurprisingly, it achieves the lowest accuracy in comparison to non-i.i.d. conditions.

Comparing *ML Mule* to the baseline methods, *ML Mule* consistently outperforms or remains competitive with them, especially as the number of rounds grows. Although skewed distributions sometimes result in lower early-stage accuracy than FedAvg or FedAS, *ML Mule* surpasses their performance in later rounds. We attribute this to the time required for the mobile device mules to ferry models between spaces and for fixed devices to wait for encounters with those mules. Despite these delays, in the later stages, the performance of *ML Mule* improves and catches up. Additionally, even during the early stages, the performance reduction is minimal.

Table 2: Accuracy Comparison Under Fixed-Device training scenario. Each block represents a different distribution strategy (Dirichlet  $\alpha = 0.001, 0.01, 0.1$  or Shards). The columns show accuracy at various rounds of model evolution (100, 200, 900). The top rows list baseline methods, while the bottom rows display results for *ML Mule* at crossing probabilities  $P_{cross} = 0, 0.1, 0.5$ . Values represent average test-set accuracy (%). Higher is better.

1	٠.	033				•		O			•	` '	O					
	Dirichlet ( $\alpha = 0.001$ )							<b>Dirichlet</b> ( $\alpha = 0.01$ )										
Round	100 200			900			100			200			900					
CFL [9]		83.12	3.12 83.97			84.12			83.05			84.31			84.27			
FedAS [8]		83.21		83.90			82.81			83.30			84.10			83.57		
FedAvg [7]		83.75 84.05			83.61			83.79			84.17			83.57				
Local Only		84.23	4.23 84.32			83.91				84.57			83.95			83.96		
$P_{cross}$	0	0.1	0.5	0	0.1	0.5	0	0.1	0.5	0	0.1	0.5	0	0.1	0.5	0	0.1	0.5
ML Mule	88.30	86.20	85.37	89.21	87.09	86.60	90.37	88.80	87.97	87.95	85.38	85.10	88.90	86.74	86.14	90.18	88.47	87.84
				Diric	hlet (α	= 0.1)								Shard	s			
Round		100		Diric	hlet (α 200	= 0.1)	<u>'</u>	900			100			Shard 200	s		900	
Round CFL [9]		<b>100</b> 72.86		Diric	•	= 0.1)		<b>900</b> 73.97			<b>100</b> 61.08				S		<b>900</b> 62.04	
				Diric	200	= 0.1)							1	200	S			
CFL [9]		72.86		Diric	<b>200</b> 74.12	= 0.1)		73.97			61.08			<b>200</b> 62.19	S		62.04	
CFL [9] FedAS [8]		72.86 72.47		Diric	<b>200</b> 74.12 73.86	= 0.1)		73.97 73.40			61.08 <b>61.32</b>			200 62.19 62.78	S		62.04 61.98	
CFL [9] FedAS [8] FedAvg [7]	0	72.86 72.47 <b>73.40</b>	0.5	Diric	200 74.12 73.86 74.17	0.5	0	73.97 73.40 73.42	0.5	0	61.08 <b>61.32</b> 60.96	0.5	0	200 62.19 62.78 62.59	0.5	0	62.04 61.98 61.89	0.5

In situations where the fixed devices in *ML Mule* receive sufficient model updates, we observe that *ML Mule* consistently outperforms existing federated and Local Only methods. We attribute this improvement to more effective clustering of the models, enabled by the movement of mobile devices (mules) providing context-aware information to the fixed devices. This context-awareness allows the fixed devices to gain a deeper understanding of their space's specific objectives, ultimately leading to better model performance.

Additionally, we observe that  $P_{cross}$  affects ML Mule's performance. A higher  $P_{cross} = 0.5$  facilitates more frequent inter-space movement, enabling devices to access a wider variety of models, but it can also introduce model instability in the early stages, as mobile devices often bring more diverse models from other spaces into the current space.

## 4.3 Evaluation with Mobile-Device Training

This section examines how ML Mule handles model training when new data primarily resides on mobile devices ( $m_a \in M$ ) that frequently move across different spaces. In these experiments, as shown in Figure 2b, the fixed devices ( $f_a \in F$ ) act solely as model holders, receiving, aggregating, and returning the model without performing any local training. Conversely, the mobile devices ( $m_a \in M$ ) exchange the model with these fixed devices and train it on their own local data.

As this setting is more aligned with fully decentralized learning than classical federated learning, we compare *ML Mule* with Gossip Learning [2], a traditional decentralized learning approach, and the Local-only method. We again use accuracy as our performance metric. We also evaluate a combination of the proposed approach with Gossip Learning, as the two approaches can operate orthogonally.

4.3.1 Experimental Setup. We first use CIFAR-100, focusing on the 20 super-classes as classification targets. Data is allocated to mules rather than fixed devices, following a Shards-like approach similar to that described above. Depending on a device's initial space, it receives 2500 images from that space's distribution (representing specialized local information) and an additional 2500 images from the fifth class in the assigned super-class (representing more general knowledge). To accommodate resource-constrained devices, we employ the same lightweight CNN model from the previous experiment. Additionally, at every time step, each mobile device acquires a new image from its current space, reflecting ongoing data generation in realistic scenarios.

As a second dataset, we use EgoExo4D [6], which is a multimodal, multi-view video dataset recorded across 13 global sites. We extract and focus on the IMU data (accelerometer and gyroscope readings), commonly used in HAR tasks. The sensor data is down-sampled at 50Hz. To handle sequential IMU data, we employ an LSTM-CNN model structure, which is well-established in HAR research [42].

To reduce simulation complexity, we focus on several distinct indoor activities from the top eight locations in EgoExo4D. Table 3 summarizes the distribution of data across spaces. Each simulation space is randomly assigned a corresponding location, and the data associated with that location is provided to the simulation space. The numbers in the table represent the number of separate data collection sessions conducted at each location for the specified activity classes. Unlike the image classification scenario, no additional data is introduced during the simulation; models evolve solely through interactions between mobile and fixed devices and retraining with the data they already have.

Table 3: Distribution of IMU data point across different locations for various activities.

Class/Location	cmu	fair	gt	iiith	indiana	sfu	uniandes	upenn
Bike Repair	72	71	109	0	107	0	0	0
Cooking	0	17	64	222	64	98	44	69
Dance	0	0	0	0	0	0	576	152
Music	0	0	0	16	49	0	0	203

At each simulation time step, Gossip Learning, and the Gossip component of ML Mule+Gossip allow mobile devices to attempt communication with surrounding mobile devices within a defined communication radius, sharing their models. We assume that it takes 3 time steps to completely share a model with neighboring devices via the peer-to-peer network. Similarly, in *ML Mule* and the Mule component of the *ML Mule* + Gossip method, mobile devices require 3 time steps to share their models with the fixed devices. These communications are limited to the fixed device assigned to the space where the mobile device is currently located. In the Local Only method, each mobile device trains its model with it's own training data for one epoch at each time slot.

In both simulations, we hold out 20% of the data for testing. Prior to the simulation, devices pretrain the model on their local data until no further improvement is observed on their local test sets. Each mule moves through the environment according to the random-walk model introduced earlier. The evaluation at any point in time is based on the data from the space where a device is currently located.

4.3.2 Results and Discussion. Figures 5 and 7 display the accuracy over time for four learning methods—Gossip, Local Only, ML Mule, and ML Mule + Gossip—under three mobility patterns characterized by  $P_{cross} = 0.5, 0.1, 0$ , using the CIFAR100 and EgoExo4D datasets, respectively. Each subfigure corresponds to one method, with the x-axis denoting simulation time and the y-axis showing the test accuracy.

To facilitate comparison from another perspective, Figures 6 and 8 reorganize the same data by plotting accuracy for different  $P_{cross}$  values, where each subfigure contains four curves corresponding to the four methods.

A consistent finding is that *ML Mule* achieves higher accuracy in most configurations, converging more rapidly and reaching better final accuracy than other baselines. The only exception appears in the very early stages, with image classification task, where Local Only can temporarily outperform *ML Mule*. This advantage quickly disappears once the decentralized methods stabilize their aggregated models. Such advantage does not exist in the results for the HAR task, as the task is more complex and it is difficult for the Local Only method to extract sufficient features from the limited data.

Mobility heavily influences the learning dynamics in this setting as well. When  $P_{cross} = 0$ , devices remain in their

initially assigned spaces, resulting in faster local convergence but reduced exposure to diverse data. In contrast, higher crossing probabilities such as  $P_{cross}=0.5$  provide more interspace travel, yielding a richer variety of model but sometimes causing the model accuracy fluctuations in early stage.

In the image classification task, both ML Mule and Gossip exhibit similar learning trajectories, though Gossip tends to converge more slowly and reaches lower peak accuracy. This discrepancy arises from the absence of a stable anchor (a fixed device) in pure Gossip, limiting its capacity to unify regional patterns. In ML Mule, mobile devices coordinate with fixed devices that hold relatively stable local models, which capture of space-specific features. By contrast, Gossip relies on device-to-device exchanges alone, which depend on the devices it encountered and the previous experience of such devices, which can lead to slower convergent. The HAR task reveals that Gossip Learning might benefits from higher mobility settings, in complex tasks, as greater device diversity improves performance. This is reflected in its better performance when  $P_{cross}$  increase, as frequent interspace interactions provide richer information from a more diverse set of encountered devices. Local Only performs well initially, as it avoids external model 'interference', but it ultimately fails to accumulate broader knowledge from the current and other spaces, leading to lower accuracy in the long run. ML Mule+Gossip performs similarly to ML Mule, suggesting that the extra peer-to-peer exchanges may not significantly improve performance once devices can already interact effectively with fixed devices.

## 5 Conclusion

This paper introduces *ML Mule*, a mobile-driven, context-aware collaborative learning framework that utilizes mobile devices to transport models between different spaces equipped with fixed devices, enabling decentralized model training in environments with limited or no internet connectivity. By relying on localized communication and mobile devices acting as "mules" *ML Mule* enables efficient model evolution without requiring centralized infrastructure. Our evaluations across two tasks—image classification with CIFAR-100 and human activity recognition with EgoExo4D—demonstrate that *ML Mule* consistently outperforms or matches baseline federated and decentralized learning methods in terms of accuracy and convergence speed.

Despite these achievements, several limitations must be acknowledged. First, *ML Mule* was tested using a simple weighted averaging aggregation strategy; exploring more advanced methods tailored for non-i.i.d. data distributions could further enhance its performance. Second, the experiments were conducted in relatively small-scale simulated environments. Deploying *ML Mule* in real-world, large-scale

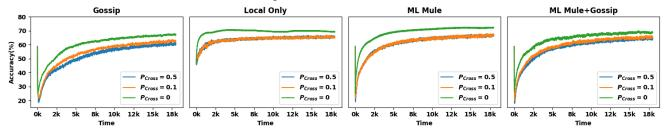


Figure 5: Accuracy over time for image classification. Each subfigure corresponds to a different method: Gossip, Local Only, ML Mule, and ML Mule+Gossip. The three curves in each subfigure represent varying crossing probabilities ( $P_{cross} = 0.5, 0.1, 0$ ). Higher  $P_{cross}$  indicates more frequent movement between spaces, while  $P_{cross} = 0$  implies no crossing. The x-axis shows simulation time and the y-axis denotes test accuracy (%).

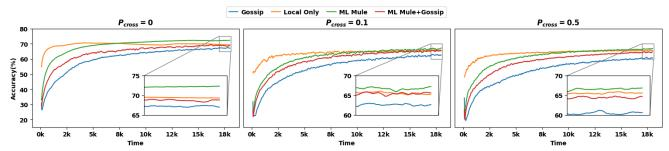


Figure 6: Accuracy over time for image classification. Each subfigure corresponds to a different ( $P_{cross} = 0.5, 0.1, 0$ ). The 4 curves in each subfigure represent varying learning method: Gossip, Local Only, ML Mule, and ML Mule+Gossip. The x-axis shows simulation time and the y-axis denotes test accuracy (%). To reduce the overlap between lines, a moving average with 100 time steps was applied to minimize the noise in the results.

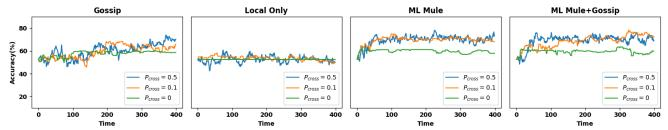


Figure 7: Accuracy over time for human activity recognition. Each subfigure corresponds to a different method: Gossip, Local Only, ML Mule, and ML Mule+Gossip. The three curves in each subfigure represent varying crossing probabilities ( $P_{cross} = 0.5, 0.1, 0$ ). Higher  $P_{cross}$  indicates more frequent movement between spaces, while  $P_{cross} = 0$  implies no crossing. The x-axis shows simulation time and the y-axis denotes test accuracy (%).

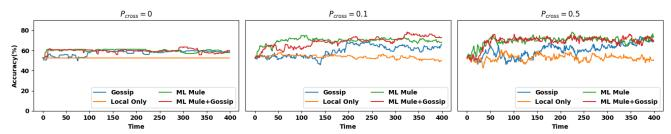


Figure 8: Accuracy over time for human activity recognition . Each subfigure corresponds to a different ( $P_{cross} = 0.5, 0.1, 0$ ). The 4 curves in each subfigure represent varying learning method: Gossip, Local Only, ML Mule, and ML Mule+Gossip. The x-axis shows simulation time and the y-axis denotes test accuracy (%).

IoT systems would require addressing additional challenges, including communication delays, hardware heterogeneity, and other resource constraints. Future researchers could expand the integration of federated learning with *ML Mule*; incorporate privacy-preserving techniques such as differential privacy or secure multiparty computation; and conduct large-scale real-world deployments testing.

In conclusion, *ML Mule* demonstrates the potential of using mobile devices as mule to carry the model in between fixed devices as a robust alternative to centralized and distributed learning in resource-constrained environments.

## References

- [1] A. Hard et al. 2018. Federated learning for mobile keyboard prediction. arXiv preprint arXiv:1811.03604.
- [2] I. Hegedűs et al. 2019. Gossip learning as a decentralized alternative to federated learning. In *Proc. of DAIS*, 74–90.
- [3] S. Lee et al. 2021. Opportunistic federated learning: an exploration of egocentric collaboration for pervasive computing applications. In *Proc. of PerCom*, 1–8.
- [4] S. Medjiah et al. 2014. Sailing over data mules in delay-tolerant networks. IEEE Transactions on Wireless Communications, 13, 1.
- [5] A. Krizhevsky et al. 2009. Learning multiple layers of features from tiny images. Tech. rep. 0. University of Toronto, Toronto, Ontario. https://www.cs.toronto.edu/~kriz/learning-features-2009-TR.pdf.
- [6] K. Grauman et al. 2024. Ego-exo4d: understanding skilled human activity from first-and third-person perspectives. In Proc. of CVPR.
- [7] B. McMahan et al. 2017. Communication-efficient learning of deep networks from decentralized data. In Artificial intelligence and statistics. PMLR, 1273–1282.
- [8] X. Yang et al. 2024. Fedas: bridging inconsistency in personalized federated learning. In *Proc. of CVPR*. (June 2024), 11986–11995.
- F. Sattler et al. 2019. Clustered federated learning: model-agnostic distributed multi-task optimization under privacy constraints. (2019). https://arxiv.org/abs/1910.01991 arXiv: 1910.01991 [cs.LG].
- [10] T.-M. H. Hsu et al. 2019. Measuring the effects of non-identical data distribution for federated visual classification. (2019). https://arxiv.org/abs/1909.06335 arXiv: 1909.06335 [cs.LG].
- [11] A. Fallah et al. 2020. Personalized federated learning: a meta-learning approach. arXiv preprint arXiv:2002.07948.
- [12] L. Yi et al. 2023. Pfedes: model heterogeneous personalized federated learning with feature extractor sharing. arXiv preprint arXiv:2311.06879.
- [13] F. Hanzely et al. 2020. Federated learning of a mixture of global and local models. arXiv preprint arXiv:2002.05516.
- [14] A. Fallah et al. 2020. Personalized federated learning with theoretical guarantees: a model-agnostic meta-learning approach. In *Advances* in *Neural Information Processing Systems*. H. Larochelle et al., (Eds.) Vol. 33. Curran Associates, Inc., 3557–3568.
- [15] J. H. Lim et al. 2024. Metavers: meta-learned versatile representations for personalized federated learning. In *Proc of WACV*.
- [16] A. Kundu et al. 2022. Robustness and personalization in federated learning: a unified approach via regularization. In Proc. of EDGE.
- [17] X. Wu et al. 2024. Decoupling general and personalized knowledge in federated learning via additive and low-rank decomposition. In Proc. of MM, 7172–7181.
- [18] H. Yu et al. 2022. Prototyping opportunistic learning in resource constrained mobile devices. In Proc. of PerCom Workshops, 521–526.
- [19] L.-M. Messmer et al. 2024. Context-aware machine learning: a survey. In *Proc. of FTC*. K. Arai, (Ed.), 252–272.

- [20] M. B. Harries et al. 1998. Extracting hidden context. Machine learning, 32. 2. 101–126.
- [21] I. H. Sarker et al. 2021. Introduction to context-aware machine learning and mobile data analytics. In Context-Aware Machine Learning and Mobile Data Analytics: Automated Rule-based Services with Intelligent Decision-Making, 3–13.
- [22] X. Wang et al. 2023. Context understanding in computer vision: a survey. Computer Vision and Image Understanding, 229.
- [23] L. Miranda et al. 2022. A survey on the use of machine learning methods in context-aware middlewares for human activity recognition. Artificial Intelligence Review, 55, 4, 3369–3400.
- [24] T. Yu et al. 2020. Learning context-aware policies from multiple smart homes via federated multi-task learning. In *Proc. of IoTDI*, 104–115.
- [25] G.-L. Huang et al. 2023. Context-aware machine learning for intelligent transportation systems: a survey. IEEE Transactions on Intelligent Transportation Systems, 24, 1, 17–36.
- [26] N. Nascimento et al. 2018. A context-aware machine learning-based approach. In Proceedings of the 28th Annual International Conference on Computer Science and Software Engineering, 40–47.
- [27] G. H. Sim et al. 2018. An online context-aware machine learning algorithm for 5g mmwave vehicular communications. *IEEE/ACM Transactions on Networking*, 26, 6, 2487–2500.
- [28] R. Liu et al. 2017. Context aware machine learning approaches for modeling elastic localization in three-dimensional composite microstructures. *Integrating Materials and Manufacturing Innovation*.
- [29] S. Menik et al. 2023. Towards modular machine learning solution development: benefits and trade-offs. (2023). https://arxiv.org/abs/23 01.09753 arXiv: 2301.09753 [cs.LG].
- [30] I. H. Sarker et al. 2020. Abc-ruleminer: user behavioral rule-based machine learning method for context-aware intelligent services. Journal of Network and Computer Applications, 168.
- [31] K. Bayoudh. 2024. A survey of multimodal hybrid deep learning for computer vision: architectures, applications, trends, and challenges. *Information Fusion*, 105.
- [32] A. Omolaja et al. 2022. Context-aware complex human activity recognition using hybrid deep learning models. Applied Sciences, 12, 18.
- [33] M. M. Bejani et al. 2018. A context aware system for driving style evaluation by an ensemble learning on smartphone sensors data. Transportation Research Part C: Emerging Technologies, 89, 303-320.
- [34] C. Wu et al. 2022. Knowledge graph-based multi-context-aware recommendation algorithm. *Information Sciences*, 595, 179–194. https://www.sciencedirect.com/science/article/pii/S0020025522001967.
- [35] O. Brdiczka. 2019. (Apr. 2019). https://business.adobe.com/blog/pers pectives/contextual-ai-the-next-frontier-of-artificial-intelligence.
- [36] E. King et al. 2023. Candor: continuous adaptive neighbor discovery. In Proc. of MASS, 336–342.
- [37] B. McMahan et al. 2017. Communication-Efficient Learning of Deep Networks from Decentralized Data. In *Proc. of AISTATS*. A. Singh et al., (Eds.) Vol. 54. (Apr. 2017), 1273–1282.
- [38] D. A. E. Acar et al. 2021. Federated learning based on dynamic regularization. In *Proc. of ICLR*.
- [39] S. P. Karimireddy et al. 2020. SCAFFOLD: stochastic controlled averaging for federated learning. In Proc. of ICML, 5132–5143.
- [40] T. Li et al. 2020. Federated optimization in heterogeneous networks. (2020). https://arxiv.org/abs/1812.06127 arXiv: 1812.06127 [cs.LG].
- [41] H. Yu et al. 2023. Idml: incentivized decentralized machine learning. arXiv preprint arXiv:2304.05354.
- [42] K. Xia et al. 2020. Lstm-cnn architecture for human activity recognition. *IEEE Access*, 8.